Modeling of Casting, Welding and Advanced Solidification Processes - XI
Edited by Charles-André Gandin and Michel Bellet
TMS (The Minerals, Metals & Materials Society), 2006

A MIXTURE TWO-PHASE MODEL FOR PREDICTING MACROSEGREGATIONS DURING SOLIDIFICATION

Yong Tang, Menghuai Wu, Andreas Ludwig

Chair for Simulation and Modeling of Metallurgical Processes
Christian–Doppler Laboratory for Multiphase Modeling of Metallurgical Processes
Department of Metallurgy, University of Leoben, A-8700 Leoben, Austria
Tel: +43 3842 402 2225, Email: yong.tong@mu-leoben.at

Keywords: Solidification, Mixture model, Macrosegregation, CFD, Multiphase Modeling

Abstract

The formation of macrosegregations during solidification is caused by the relative motion between melt and growing solid. Recently, Eulerian multiphase approaches came up to describe this relative motion. Because conservation equations must be solved for each considered phase, the Eulerian approaches have high computation costs. In order to reduce these costs, a mixture model is suggested in this paper. For the mixture phase only one single momentum and enthalpy equation has to be solved. A so-called drift flux model handles the relative motion between the liquid and the solid. In addition, mass and species conservation are solved for each phase. Grain nucleation and transport is considered with a suitable number density conservation equation. It turned out, that the major features of an Eulerian approach remains, but the calculation costs are reduced and the solution procedure is more stable. The model is applied for the solidification of a cylindrical steel ingot casting. The results indicate that the mixture model can be practically used to simulate large ingot casting at industry scale by making full use of the advantages of the CFD technology in terms of sophisticated solidification modeling details.

Introduction

With the advances in numerical simulation technology and in computer power, it is nowadays possible to perform multiphase flow calculations for solidification processes. The consideration of flow in a casting process provides the possibility of predicting macrosegregations. At the beginning, only a single phase was considered. Hills et al. [1], Prantil and Dawson [2], and Bennon and Incopera [3] employed the concept of mixture to derive macroscopic transfer equations without any microscopic consideration. Based on the averaging procedure for multiphase systems [4-8], Ni and Beckermann developed a volume-averaging two-phase model to describe transport phenomena during solidification [9]. In this volume-averaging two-phase model the number density of crystal is introduced and the solid fraction is mathematically derived from the solid continuity equation. Meanwhile, the concept of mixture is still used in many solidification simulations for computational convenience. Ni and Incropera[10] developed a so called “extension of the continuum model” by keeping the features of volume-averaging two-phase model and enabling its ability to treat solutal undercooling, nucleation, stereological characteristics of the solid/liquid interface, solid movement in the form of floating or settling crystals, and shrinkage. Gu [11] has done some calculations of convection and formation of macrosegregations for large steel ingots based on Schneider’s[12] work. His mathematical model was also based on the concept of mixture and no extra solid movement in the liquid zone was considered. Thus, sedimentation of equiaxed grains was not considered. Recently, Ludwig and Wu [13, 19] presented numerical simulations of globular equiaxed solidifications with a volume-averaging two-phase approach. In

this simulation, both liquid and solid (globular equiaxed grains) are taken as separated but highly coupled interpenetrating continua. The conservation equations for mass, momentum, species mass fraction and enthalpy are solved for both phases. Oldfield's approach [14] for heterogeneous nucleation was used. This solidification model can describe the grain movement and formation of negative macrosegregation caused by grain sedimentation. However, in the application of this model to large size ingot casting, the computation costs are still too high although the computer power has increased significantly in recent years. One reason for the high calculation costs is that the momentum conservation equation for each individual phase has to be solved. The mixture model introduced in this paper employed all the important features like nucleation, species transfer due to solute redistribution, mass transfer from liquid to solid etc. as used in the previous Wu and Ludwig model[13,19], except that the concept of mixture is applied for enthalpy and momentum. The derivation of this mixture model is based on the work of Manninen et al. [15]. The solution procedure for this model turned out to be quite stable and the necessary computational costs are reduced.

Mathematical Model

Model assumptions

The following assumptions were made:

(1) Two phases are considered, liquid (primary phase) and solid (secondary phase). They are treated as interpenetrating continua and so their volume fractions sum up to one, $f_l + f_s = 1$. The solid phase is considered to represent globular equiaxed grains with an ideal spherical shape. The mixture phase is defined as an artificial phase consisting both liquid and solid. Its properties depend on the phase fraction.
(2) The volume-averaging method is applied to all variables used in the conservation equations.
(3) After the solid grains are generated in the melt, local mechanical equilibrium between the moving grains is achieved over short spatial length scales. The local equilibrium approximation requires that a grain is rapidly accelerated to the terminal velocity.
(4) Thermodynamic equilibrium is assumed to exist at the solid/liquid interface.
(5) In a control volume, only one single temperature for the mixture is referred.

Conservation equations

Continuity equation for the mixture: by summing up the continuity equations of the liquid and the solid as given in the full Eulerian approach, the continuity equation of a solid/liquid mixture is obtained as

$$\frac{\partial \rho_m}{\partial t} + \nabla \cdot (\rho_m \vec{u}_m) = 0, \tag{1}$$

where a mixture density, ρ_m, and a mixture velocity, $\vec{u}_m$, is defined by

$$\rho_m = f_l \rho_l + f_s \rho_s, \tag{2}$$

$$\vec{u}_m = \frac{f_l \rho_l \vec{u}_l + f_s \rho_s \vec{u}_s}{\rho_m} = w_l \vec{u}_l + w_s \vec{u}_s. \tag{3}$$

In Eq. (3), $w_i = f_i \rho_i / \rho_m$ stands for the mass fraction of phase $i = l$ or s.

Momentum equation for the mixture: the momentum conservation equation for the mixture is derived again by summing up the individual momentum conservation equations as given in the full Eulerian approach. This gives

$$\frac{\partial}{\partial t}\rho_m \vec{u}_m + \nabla\cdot(\rho_m \vec{u}_m \vec{u}_m) = -\nabla p + \nabla\cdot(\tau_m + \tau_{Tm}) + \nabla\cdot\tau_{Dm} + \rho_m \vec{g}\,, \tag{4}$$

where it is assumed that the liquid and the solid share the some pressure field. The three stress tensors are defined by

$$\tau_m = f_l\tau_l + f_s\tau_s\,, \tag{5}$$

$$\tau_{Tm} = -(f_l\rho_l\overline{\vec{u}_{Fl}\vec{u}_{Fl}} + f_s\overline{\rho_s\vec{u}_{Fs}\vec{u}_{Fs}})\,, \tag{6}$$

$$\tau_{Dm} = -(f_l\rho_l\vec{u}_{Ml}\vec{u}_{Ml} + f_s\rho_s\vec{u}_{Ms}\vec{u}_{Ms})\,. \tag{7}$$

τ_m represents the average viscous stress, τ_i the viscous stress of phase *i*, τ_{Tm} the turbulent stress and τ_{Dm} the diffusion stress due to the phase slip. $\vec{u}_{Ml} = \vec{u}_l - \vec{u}_m$ and $\vec{u}_{Ms} = \vec{u}_s - \vec{u}_m$ are the drift velocities of *l* and *s*. $\vec{u}_{Fi}$ is the fluctuating component of the velocity for phase *i* e.q. $\vec{u}_{Fi} = \vec{u}_{Ii} - \vec{u}_i$, with $\vec{u}_{Ii}$ denoting the local instant velocity of phase *i*. The over bars in Eq. (6) indicate an average inside same averaging volume. The term $\nabla\cdot\tau_{Dm}$ in Eq. (4) represents the momentum diffusion due to the relative motion.

Similar to the approach used in the Eulerian model for equiaxed solidification proposed earlier be two of the present author[13,19], it is assumed that an artificial viscosity of the solid phase can be introduced which accounts for the increase of the effective viscosity of a solid/liquid mixture with solid fraction. This solid viscosity is expressed by [17]

$$\mu_s = \frac{\mu_l}{f_s}\cdot\left(\left(1 - f_s/f_s^c\right)^{-2.5\cdot f_s^c} - \left(1 - f_s\right)\right). \tag{8}$$

Here, f_s^c assumed to be the packing limit, $f_s^c = 0.637$. For $f_s > f_s^c$, μ_s is infinitely large.

In practice, the drift velocity is determined by the relative velocity between the two phases which is also known as slip velocity, $\vec{u}_{l-s} = \vec{u}_s - \vec{u}_l$. Note that the drift and slip velocities are related to each other by

$$\vec{u}_{Ms} = (1 - w_s)\cdot\vec{u}_{l-s}\,. \tag{9}$$

Due to the assumption of local mechanical equilibrium, the relative velocity between liquid and solid can be expressed according to Manninen et al.[15] by

$$\vec{u}_{l-s} = \frac{\tau_s}{f_{drag}}\frac{(\rho_s - \rho_m)}{\rho_s}\vec{a}_s\,. \tag{10}$$

Here, τ_s is a relaxation time, f_{drag} the drag function and $\vec{a}_s$ the acceleration of the grains. As we assume that $\mathrm{Re}_s < 1$ (Stokes regime), the relaxation time is given by $\tau_s = \rho_s d_s^2/(18\mu_l)$ [15], with d_s being the (volume averaged) diameter of the solid phase. As in ref. [13], we assume that the drag between the grains and the melt can be described by Kozeny-Karman below the packing limit (submerged object approach) and by Blake-Kozeny above the packing limit (porous medium approach). Thus, we applied

$$f_{drag} = \begin{cases} \dfrac{10 \cdot f_s}{f_l^2} & f_s \le f_s^c \\ \dfrac{d_s^2 \cdot f_s}{18 \cdot K_0 \cdot f_l^2} & f_s > f_s^c \end{cases} \tag{11}$$

To obtain a continuous transition we chose the empirical permeability parameter K_0 to be $K_0 = d_s^2/180$ at $f_s = f_s^c$ which was then kept constant for $f_s > f_s^c$.

The acceleration of the grains, $\vec{a}_s$, used in Eq. (10) is of the form

$$\vec{a}_s = \vec{g} - (\vec{u}_m \cdot \nabla)\vec{u}_m - \frac{\partial \vec{u}_m}{\partial t} \tag{12}$$

In this simulation, the acceleration of the globular equiaxed grain is given by gravity. Here, the grains slip velocity is first solved by the above algebraic method, then the relation between drift velocity and slip velocity determines the drift term τ_{Dm} in Eq. (4). There are also closure relations for the terms τ_m, τ_{Tm}. Detailed deduction can be found in Manninen et al's work[15]. As the momentum equation, Eq. (4), is closed, the mixture velocity can be estimated. From the mixture and slip velocities, the individual velocity of the liquid and the solid is obtained.

Volume fraction equation for the secondary phase: from the continuity equation of solid phase in the full Eulerian approach, the volume fraction of solid can be estimated as

$$\frac{\partial}{\partial t}(f_s \rho_s) + \nabla \cdot (f_s \rho_s \vec{u}_m) = M_{ls} - \nabla \cdot (f_s \rho_s \vec{u}_{Ms}) . \tag{13}$$

Here, the definition of drift velocity is used to eliminate the phase velocity. In order to define the net mass transfer rate, diffusion controlled grain growth kinetics is assumed. Thus, the growth velocity in the radius direction, v_{R_e}, can be solved analytically to give

$$v_R = \frac{dR}{dt} = \frac{D_l}{R} \cdot \frac{c_l^* - c_l}{c_l^* - c_s^*} = \frac{D_l}{R(1-k)} \cdot \left(1 - \frac{c_l}{c_l^*}\right). \tag{14}$$

c_l^* and c_s^* are the equilibrium liquid and solid concentrations adjacent to the solid/liquid interface, for which $c_s^* = k c_l^*$ (with a constant redistribution coefficient k) and $c_l^* = (T - T_f)/m$ yields. D_l is the diffusion coefficient in the liquid. The volume-averaged radius of equiaxed grains, $R = d/2$, is calculated according to $f_s = n \cdot \frac{4\pi}{3}(d/2)^3$. With Eq. (14) we can define the volume-averaged net mass transfer rate for the globular equiaxed solidification by considering the total surface area of spherical grains and taking the impingement by an Avrami-factor f_l into account. So we get

$$M_{ls} = v_R \cdot \left(n \cdot \pi d_s^2\right) \cdot \rho_s \cdot f_l \tag{15}$$

and,

$$M_{ls} = \frac{D_l}{(d/2) \cdot (1-k)} \cdot \left(1 - \frac{c_l}{(T - T_f)/m}\right) \cdot \left(n \cdot \pi d^2\right) \cdot \rho_s \cdot f_l . \tag{16}$$

Enthalpy conservation equation for the mixture: the enthalpy conservation equation for the mixture takes the following form

$$\frac{\partial}{\partial t}(f_l\rho_l h_l + f_s\rho_s h_s) + \nabla\cdot(f_l\rho_l\vec{u}_l h_l + f_s\rho_s\vec{u}_s h_s) = \nabla\cdot(K_{eff}\nabla T) + Q\,, \tag{17}$$

where $K_{eff} = f_l K_l + f_s K_s$ is the effective conductivity and Q the heat source (sink) caused by the releasing of the latent heat during the solidification or solid re-melting if the same heat capacity for the liquid and solid phase are assumed .

Species conservation for each phase: the species conservation equation for each phase is given as

$$\frac{\partial}{\partial t}(f_l\rho_l c_l) + \nabla\cdot(f_l\rho_l\vec{u}_l c_l) = \nabla\cdot(f_l\rho_l D_l\nabla c_l) + C_{sl}\,, \tag{18}$$

$$\frac{\partial}{\partial t}(f_s\rho_s c_s) + \nabla\cdot(f_s\rho_s\vec{u}_s c_s) = \nabla\cdot(f_s\rho_s D_s\nabla c_s) + C_{ls}\,, \tag{19}$$

Where, $C_{ls}(=-C_{sl})$ denotes the species exchange rate between both phases defined elsewhere [13].

Grain number density conservation equation: the conservation of the grain number density, n, is expressed in the following scalar conservation equation

$$\frac{\partial}{\partial t}n + \nabla\cdot(\vec{u}_s n) = N\,. \tag{20}$$

The nucleation rate, *N*, was deducted from Oldfield's approach [14] which assumes that the heterogeneous nucleation takes place at different classes of sites.

The equations to model globular equiaxed solidification solved in the mixture model are show in figure 1.

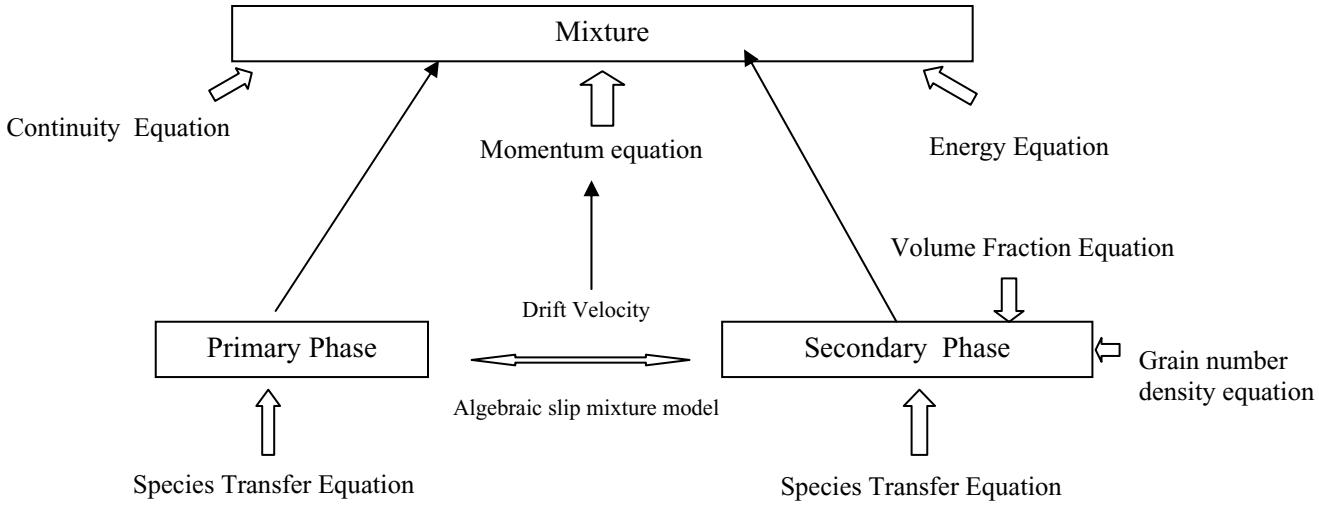

Figure1. Considered conservation equations in the mixture model.

Simulation and Results

Introduction of the simulation case

A benchmark cylindrical ingot with simple geometry was simulated with the proposed mixture model. As casting alloy binary carbon steel with 0.34 wt % carbon is considered. The initial casting temperature was assumed to be $T_0 = 1800$ K and the initial composition of the melt $c_0^C = 0.34$ wt. %. The velocities of liquid and solid are initially set to zero. A 2D axis-symmetrical computation domain was chosen to simulate the cylindrical ingot. Boundary conditions, initial casting parameters, grids and geometry sizes of this benchmark ingot are shown in Figure.2. The size of a volume element within the square grid was chosen to be 1.25 mm^2. The simulation was implemented into the commercial CFD code FLUENT 6.2.16. Time steps for the calculation were between 0.001s and 0.05 s. About ten hours of computing time was needed on one single PC cluster node with 3.2GHz.

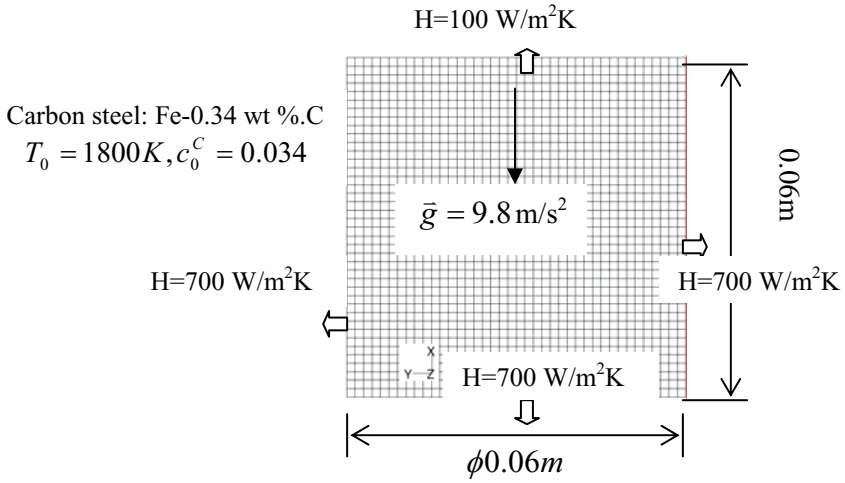

Figure 2. Scheme of computing domain and boundary conditions

Results and Discussion

As the purpose of this paper is to evaluate the consistence of the proposed mixture model, we do not intend to reproduce reality. In a real steel ingot casting, we would expect columnar dendrites and equiaxed grains. However, in our model only globular equiaxed grains with an ideal spherical shape are considered at present.

Figure 3. shows the temperature fields during the solidification of the ingot. A logical evaluation sequence of the temperature fields is obtained, although the mixture model solves the energy conservation equation only on the mixture level. These results indicate that the mixture model is more efficient regarding to the calculation cost than the Eulerian approach which solves energy conservation equations for all phases considered.

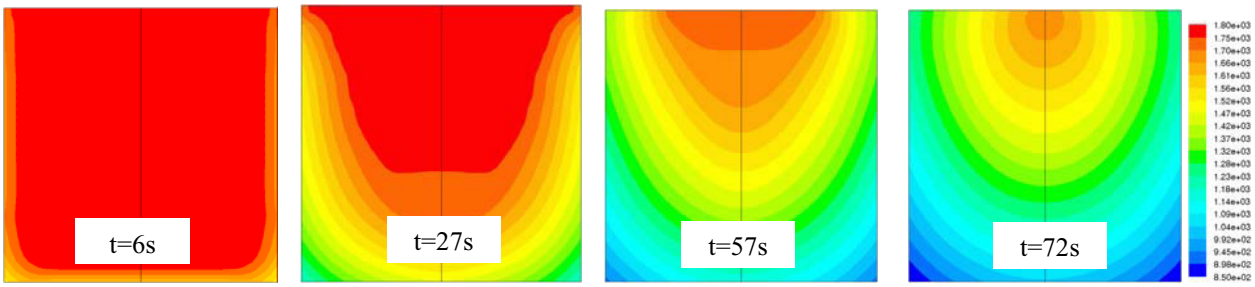

Figure 3. Evolution of temperature fields during solidification (850~1800 K).

The solidification process is shown in Figure.4. For the mixture model, the most important thing is to derive the velocity of the secondary phase since no separate momentum conservation equation is solved for the velocity field of secondary phase. According to the rules for proper application of the mixture model suggested by FLUENT, the mixture model is applicable in the multiphase system if the Stokes number S_t of the secondary phase is less than one. For the steel, the density of secondary phase ρ_d = 7200 kg/m^3, the viscosity of liquid melt μ_c = 0.006 kg/ms, the characteristic length of most steel castings L_s = 0.1~1 m, and the characteristic velocity V_s = 0.001~0.1 m/s, thus by assuming spherical morphology of the secondary phase the Stokes number can be approximated as

$$St = \frac{\rho_d d_p^2}{18\mu_c} \cdot \frac{V_s}{L_s} = 0.000067 \sim 0.67 < 1. \tag{21}$$

It means that the mixture model applies for the steel castings, and it does not lose its availability in the velocity field.

Figure.4 shows the different velocity fields of liquid and solid phases during solidification. At the beginning (t = 6 s), most of the solid crystals have the similar velocity field to the liquid phase except for the area near the top of the ingot where solid grains fall downwards. As the solidification proceeds (t = 27s, t = 57s), most of the solidified grains will sedimentate and settle in the bottom of the ingot because of the higher density of the solid grains. These predictions agree quite well with the experimental observation of solidification. One interesting thing here is that at the final stage of solidification (t = 72s), the liquid phase in casting centre flows downwards rather than upwards as seen in the previous pictures. The explanation is that such kind of liquid flow is induced by the wide density change of solid and liquid phases at the end of the solidification.

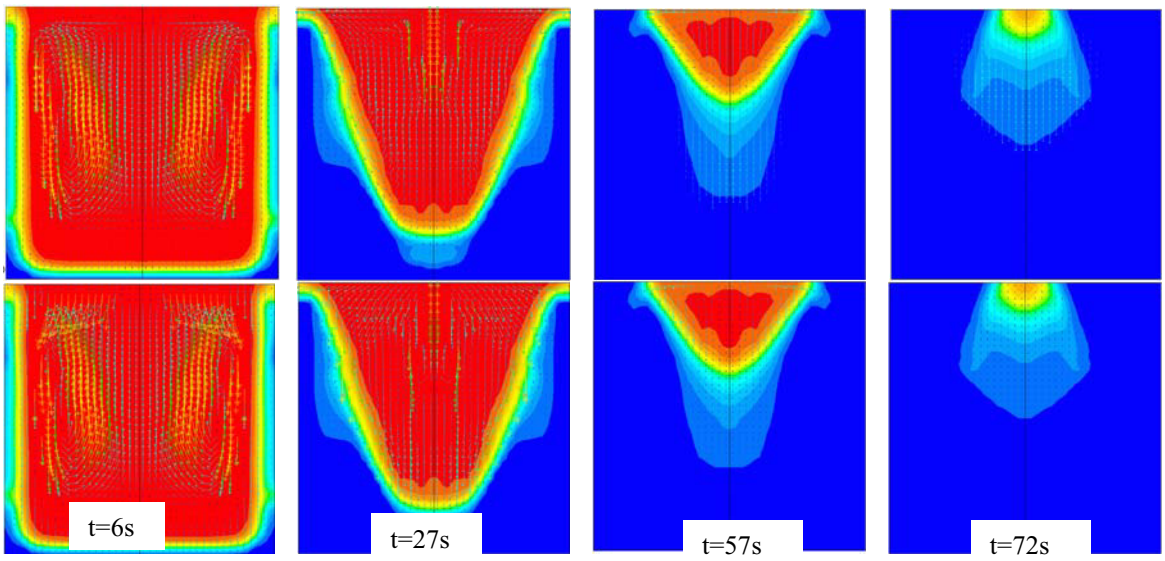

Figure 4. Evolution of solid fraction together with the velocity of liquid steel (above) and the velocity of grains (low) ($\vec{u}_{\max} = 0.01\ m/s$)

The mix carbon concentration ($c_{mix}^C = \frac{c_l^C \cdot \rho_l \cdot f_l + c_s^C \cdot \rho_s \cdot f_s}{\rho_l \cdot f_l + \rho_s \cdot f_s}$) in the ingot during the solidification process is shown in Figure 5. Positive macrosegregation is observed near the top and centre bottom areas of the ingot. Because of the solute partition during solidification (partition coefficient of carbon in the steel is lees than one), the carbon concentration in the melt arises with solidification. Finally, when the liquid steel with higher carbon content solidifies, the solid phase at the end of solidification will have very high concentration as shown in this figure. The negative seg-

regations, as illustrated with blue color in Figure 5, are caused by grain sedimentation. In this mixture model the density of liquid phase changes with the temperature and concentration, and the densities of the liquid and solid are different. The density change can cause some kinds of feeding phenomena. If the ingot is not 100% perfectly solidified, the flow with high carbon concentration can penetrate into partly solidified (or not 100% perfectly solidified) area and cause the mix concentration changing during the solidification. This can explain the mix concentration change in the partly solidified areas during the solidification in Figure 5.

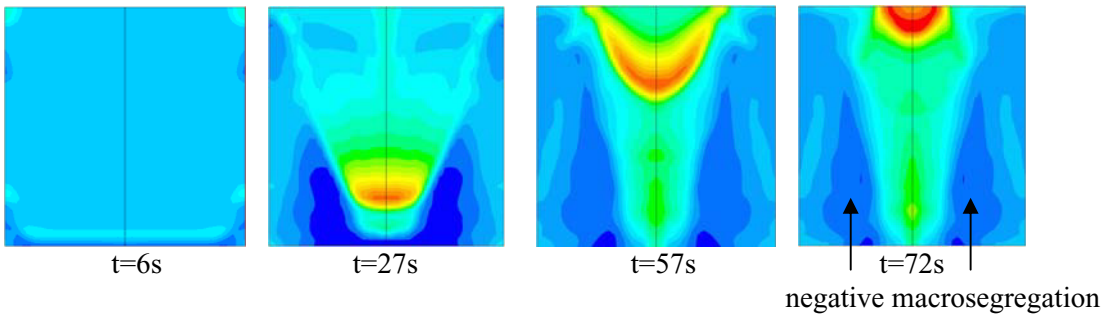

Figure5. Carbon concentration change (c_{mix}) during the solidification. The values are in the range from 0.14 to 1.3 wt. % during the solidification.

Conclusions

A mixture model for globular equiaxed solidification considering nucleation, grain growth and motion, sedimentation, thermo-solutal melt convection and the formation of micro- and macrosegregations was presented. A binary steel ingot casting was simulated as benchmark. The predicted solidification sequence and the formation of macrosegregations are encouraging. Compared to the full Eulerian approach the mixture model saves computing time. With further improvement such as including columnar dendrites, the formation of shrinkage cavities and predictions on porosity, the mixture model might be suitable for describing industrial scale ingot castings.

References

1. R.N. Hills, D.E. Lopper, and P.H. Roberts, *Q. J. Mech. Appl. Math.*, 36 (1983),505-536.
2. V.C. Prantil, P.R. Dawson, *Transport Phenomena in Materials Processing* (ASME, New York, **NY,** 1983) ,469-484.
3. W.D. Bennon, F.P. Incropera, *Int. J. Heat Mass Trans.*, 20 (1987), 2161-2170.
4. D.A. Drew, *Ann. Rev. Fluid Mech*., 15 (1983) ,261-291.
5. M. Ishii, *Thermo-Fluid Dynamic Theory of Two-Phase Flow*, (Eyrolles, Paris, 1975).
6. W.G. Gray, *Adv. Water Resour*., 16 (1983), 130-140.
7. S. Ganesan, D.R. Poirier, *Metall. Trans. B*, 21 (1990) ,173-181.
8. W.G. Gray, K. O'Neill, *Water Resour. Res*., 12 (1976), 148-154.
9. J. Ni, C. Beckermann, *Metall. Trans. B*, 22 (1991) ,349-361.
10. J. Ni, F.P. Incropera, *Int. J. Heat Mass Transfer,* 38 (1995) ,1271-1284.
11. J.P. Gu, C. Beckermann, *Metall. Trans. A,* 30 (1999),1357-1366.
12. M.C. Schneider, C.Beckermann, *Metall. Trans. A,* 26 (1995) ,2373-2388.
13. A. Ludwig, M. Wu, *Metall. Trans. A,* 33 (2002), 3673-3683.
14. W. Oldfield, *Trans. ASM*, 59 (1966), 945-961.
15. M. Manninen, V. Taivassalo, and S. Kallio, "On the Mixture model for Multiphase Flow" (VTT publications 288, Finland, 1996).
16. L. Schiller, Z. Naumann, *Z. Ver. Deutsch. Ing.*, 77 (1935), 318.
17. M. Ishii, N. Zuber, *AIChE J.*, 25 (1979) ,843-855.
18. T.U. Kaempfer, M. Rappaz, *Proc. 9th Conf. on 'Modeling of casting, welding and advanced solidification processes'*, Aachen, Germany, TMS, (2000) ,640-645.
19. M. Wu, A. Ludwig, et al., *Int. J. Heat Mass Trans.*, 46 (2003), 2819-2832.